String-level modeling of two, three and four terminal Si-based tandem modules

Henning Schulte-Huxel, Daniel J. Friedman and Adele C. Tamboli

***Abstract*— III-V/Si tandem solar cells have demonstrated efficiencies exceeding the theoretical efficiency limit of silicon solar cells. On the cell level, device modeling shows that three-terminal tandem (3T) devices with rear contacted bottom Si cells perform as well as operating the subcells independently (4T). However, integrating these 3T devices in a module requires voltage matching of the top and the bottom cell. Here, we investigate the robustness of parallel/series interconnected 3T III-V/Si tandem devices in comparison with series interconnected two terminal (2T) and independently operated (4T) devices with respect to spectral, thermal, and resistive effects. Under most conditions, interconnected 3T devices are able to perform as well as those with independent operation of the top and bottom cell, and 3T devices significantly outperform 2T devices.**

***Index Terms*—Tandem device, multi-junction solar cells, module interconnection, silicon solar cell**

I. Introduction

Due to their demonstrated efficiencies exceeding the theoretical limit of single junction solar cells, III-V/Si tandem solar cells have been a focus of research in the recent years, and have reached efficiency records of over 32% [1]. These results can be achieved using either GaAs or GaInP top cells, which feature band gaps of 1.42 eV and 1.81 eV, respectively. Depending on the design of the subcells and the bonding technique, different configurations of the tandem cells are possible, i.e., a tandem cell featuring two, three, or four terminals [2].

Two terminal (2T) devices have the advantage that for module integration, they can be interconnected in series, as with single junction devices (Fig. 1 a). However, series interconnection requires current matching of the subcells. This current matching results in a strong restriction of the band gap of the top cell and causes significant performance losses under varying spectra [2–4]. Operating the two subcells independently, as in the case of four terminal (4T) devices [2, 4, 5], circumvents current matching, as shown in Fig. 1 c). However, this results in more complex system integration.

Device modeling has predicted that three terminal (3T) devices perform as well as 4T devices, and the effects on the device performance due to extracting power from the two different subcircuits of the bottom cell are marginal [6, 7].3T devices can have benefits in cell processing and interconnection. In this design, Si cells with an interdigitated back contact (IBC) design and a conductive front surface field can be used to enable tandem cells that do not require intermediate grids.

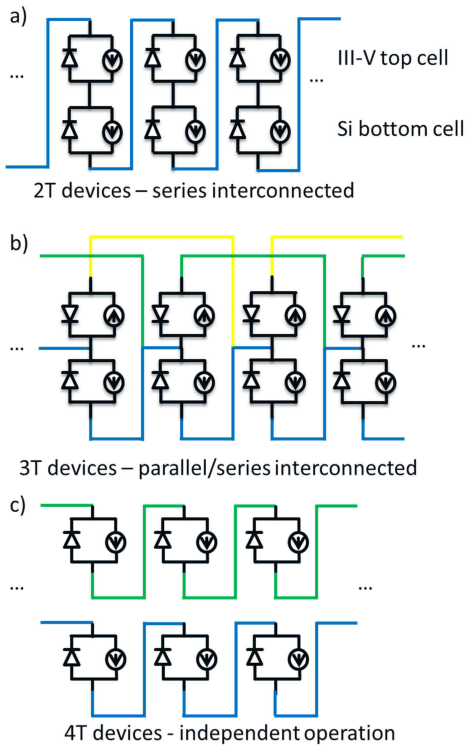

Fig. 1 Schemes of the interconnection of a) 2T, b) 3T, and c) 4T tandem cells. 2T devices are limited by current matching of the subcells, and interconnected 3T devices are limited by matching of the voltages in the substrings of top and bottom cells.

H. Schulte-Huxel acknowledges support for the Research Fellowship by Deutsche Forschungsgemeinschaft (DFG) (grant agreement No: SCHU 3206/1-1). Funding for this work at NREL was provided by DOE through EERE contract SETP DE-EE00030299 and under Contract No. DE-AC36-08GO28308.

Henning Schulte-Huxel was with the National Renewable Energy Laboratory, 15013 Denver West Parkway, Golden, CO 80401, USA and is now with the Institute for Solar Energy Research Hamelin (ISFH), Emmerthal 31860, Germany (h.schulte@isfh.de).

Daniel J. Friedman and Adele C. Tamboli are with the National Renewable Energy Laboratory, 15013 Denver West Parkway, Golden, CO 80401, USA (e-mail: adele.tamboli@nrel.gov, daniel.friedman@nrel.gov)

Pursuant to the DOE Public Access Plan, this document represents the authors' peer-reviewed, accepted manuscript. The published version of the article is available from the relevant publisher.

Nevertheless, the parallel/series interconnection of 3T devices in modules, shown in Fig. 1b, requires that the voltages of series connected bottom cells (e.g. two) are matched with the voltage of one top cell. This requirement of voltage matching also applies to the 4T devices integrated into modules featuring only two external contacts [2]. However, past studies have mainly focused on the performance of individual devices [4, 8]. There are few works that compare interconnected tandem cells, [2] which typically focus on special configurations to reach current or voltage matching conditions [9–12].

In this work, we investigate the robustness of parallel/series interconnection 3T III-V/Si tandem devices in comparison with series interconnected 2T devices and independently operated 4T devices with respect to spectral, thermal, and resistive effects. We take into account the restriction for 3T devices that the ratio of the number of bottom cells to the number of top cells interconnected in parallel is an integer, since other configurations require a more complicated interconnection scheme.

This is an extended work of our recent contribution presented at the 44rd IEEE PVSC [13]. We significantly expanded the investigation by adding the impact of changes in illumination intensity, annual yield calculations and resistive effects.

II. Simulation Model

We use the 1D ideal diode model of a solar cell in order to model the theoretical efficiency for the III-V/Si tandem cell with varying band gap E_g of the top cell. As input parameters for the top and the bottom cell, we use the dark saturation current density J_0 and the short circuit current density J_{sc}.

J_0 of the top and bottom is based on an empirically determined difference between E_g and the open circuit voltage V_{oc} of W_{oc} = 0.4 eV at 25°C [14]. This W_{oc} is good approximation for III-V materials with bang gaps between 1.1 eV and 2.1 eV [15], even though GaAs and GaInP reach lower values [16]. We calculate J_0 by

$$J_0 = J_s \exp(-qV_{oc}/nkT), \quad (1)$$

with a standard current density J_s of 16 mA/cm² [14] and an ideality factor n of unity. We implement the temperature dependence of J_0 through [17]

$$J_0(T) \sim T^3 \exp(-E_g(T)/kT), \quad (2)$$

using J_0 at 25°C as reference. The temperature dependence of $E_g(T)$ is calculated using the Varshni coefficients of Si for the bottom cell [18] and of GaAs for the top cell [19], which is used as representative material for a direct band gap III-V semiconductor. For simplicity, we use the linear approximation of the Varshni coefficients of GaAs between -40°C and 80°C.

The short circuit current density J_{sc} of the top cell is determined by using the Beer–Lambert law and the spectral dependent absorption coefficient of GaAs [20], serving again as representative material, shifted by the difference of the band gap edge with respect to GaAs at 25°C. J_{sc} for the bottom cell is determined by using the spectral dependent absorption coefficient of Si [21] and the transmission of the top cell assuming no reflection at the interface. The thickness of the III-V top cells is assumed to be 1 µm. This is for example the total GaInP thickness in the 1.81 eV GaInP record solar cell [16]. The optimal band gap of the subcells for multijunction devices may depend significantly on the cell thicknesses and other material properties [14]. For the Si bottom cell, we assume slight light trapping resulting in an effective optical thickness of 1 mm. We use the AM 1.5G spectrum (ASTM G-173-03) and the AM1G to AM10G spectra calculated by SMARTS 2.95 [22, 23] (average photon energy of the used spectra of 1.84 – 1.58 eV for 280 – 1200 nm). Losses due to parasitic absorption, reflection, shading, and resistances are not taken into account unless stated otherwise. Luminescent coupling of the junctions is assumed to be negligible.

In case of the interconnection of 3T devices, the power of individual cells at the string ends is partially lost [2]. Depending on the cell design, the power loss is on the order of the power of one tandem cell, i.e., for 60 cell string this corresponds to a 1.6% loss. For simplicity, these losses are neglected in this work by assuming an infinite string.

III. Results and Discussion

Fig. 2 shows the evolution of the efficiency for a III-V/Si tandem solar cell under standard testing conditions (STC, 1000 W/m², AM1.5G, 25°C) operating the top and bottom cells independently, series interconnected (2T devices), or parallel/series interconnected (3T devices). In the case of parallel/series interconnected 3T devices, we assume one top cell interconnected in parallel to a series of one, two, or three bottom cells, denoted as 1:1, 1:2, and 1:3, respectively. Operating the cells independently (black curve) leads to the highest efficiency for all band gap energies of the top cell, with a maximum efficiency η_{max} of 37.8% at E_g = 1.81 eV, which corresponds to the band gap of GaInP cells [16]. In case of the series interconnected 2T devices (green curve), η_{max} is 37.4% at 1.67 eV. For parallel/series interconnected 3T devices, the ratio of 1:1 (cyan curve) leads to η_{max} = 26.9%, which is approximately the same as the efficiency calculated for the bottom Si cell. This is caused by the fact that the voltage of the Si cell limits the device voltage, and in our model, every absorbed photon leads to an electron-hole pair. In case of a ratio of 1:3 (blue curve), an efficiency of 34.1% is predicted at E_g = 2.36 eV. This is well below the efficiency of the parallel/series interconnected 3T devices with a ratio of 1:2 (red curve), with η_{max} = 37.8% at E_g = 1.80 eV, almost identical to the result for independent operation. This shows

Pursuant to the DOE Public Access Plan, this document represents the authors' peer-reviewed, accepted manuscript. The published version of the article is available from the relevant publisher.

that the conclusion that individual 3T devices operating as well as 4T devices can also hold for modules with two terminals, if a suitable top cell band gap is chosen.

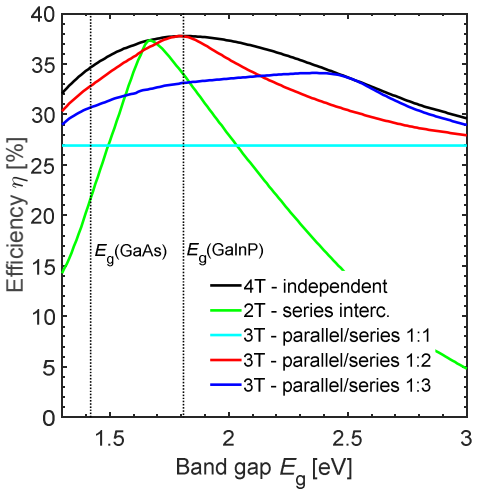

Fig. 2 Efficiency under STC for III-V/Si tandem solar cells using different operation modes as a function band gap of the top cell. The band gap energies of GaAs and GaInP are indicated by vertical lines.

The thickness of the subcells can have an impact on the optimal bandgap of the top cell as well as on the maximum efficiency. As an example, the variation of the top cells thickness d_{top} is shown in Fig. 3. With increasing thickness d_{top} the fraction of light absorbed in the top cell increases and, since the dark saturation current density J_0 in this work depends only on the bandgap, the efficiency is also affected. As the current absorbed by the top cell is delivered at a higher voltage than by the bottom cell, the efficiencies of the different configurations of tandem devices increases for increasing top cell thickness as shown in Fig. 3 b).

In case of current-matched 2T devices, the optimal band gap shifts from 1.31 eV for a top cell thickness of 0.2 µm to 1.8 eV for an infinitely thick top cell as shown in Fig. 3 c). In addition, the band gap for the 4T devices shifts from 1.77 eV to 1.86 eV for a 0.2 µm and infinitely thick top cell, respectively. For 3T devices, the impact of d_{top} on the optimal bandgap is small, i.e., for d_{top} between 0.5 µm and 10 µm the optimal band gap is 1.80 eV, for 0.2 µm it is 1.82 eV and for an infinitely thick top cell 1.79 eV. However, for real devices the thickness dependence will be quite different, due to a decrease in W_{oc} for thicker cells [16] and, with realistic diffusion lengths, the current enhancement may not be proportional to the increase in absorption. For this work, we keep the thickness of the top cell constant at 1 µm for the following investigations, which is typical for GaInP top cells. The general trends shown here are expected to be valid for different thicknesses of the subcells.

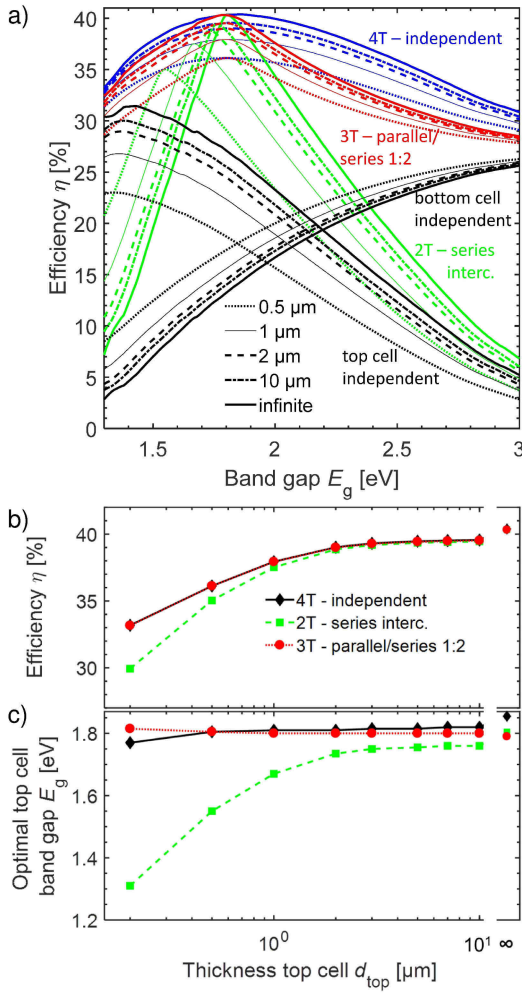

Fig. 3 a) Efficiency under STC of III-V/Si tandem solar cells for different top cell thickness and operation modes, as a function of the band gap of the top cell. b) and c) show the maximum efficiencies and the corresponding optimal top cell band gap for the different operation modes as function of the top cell's thickness.

A. *Changes in illumination spectra*

Changes in the illumination spectra have significant impact on the performance of tandem solar cells, since the ratio of currents generated in the top and bottom cell is affected, and the two cells work at different voltages at maximum power point. The optimum band gap of the top cell and the corresponding maximum efficiencies η_{max} of the simulations are shown in Fig. 4 a) for different spectra at constant illumination intensity of 1000 W/m². The series interconnected devices show a significant decrease in the optimal band gap from 1.70 eV to 1.46 eV when changing from AM1G to AM10G.

In contrast to this, for parallel/series interconnected 3T (1:2) devices, the optimal band gap is almost unaffected by spectral changes and constant at 1.80eV. As shown in Fig. 4 b), the consequence is that 3T devices are very robust to spectral changes and perform as well as operating the subcells independently.

Pursuant to the DOE Public Access Plan, this document represents the authors' peer-reviewed, accepted manuscript. The published version of the article is available from the relevant publisher.

Changes in the spectrum tend to occur together with changes in intensity. In case of the independent operation or series interconnection of the sub cells, the optimal band gap is unaffected by changes in illumination intensity. This is caused by the fact that the current scales linearly with intensity for both subcells. According to (1), the open-circuit voltage and thus also the voltage at maximum power point depend on the short circuit current. In the case of the parallel/series interconnected 3T (1:2) device, the sum of the voltages of the two bottom cells decreases more than of the top cell. Thus, the optimal band gap of the top cell decreases slightly, from 1.80 eV to 1.75 eV.

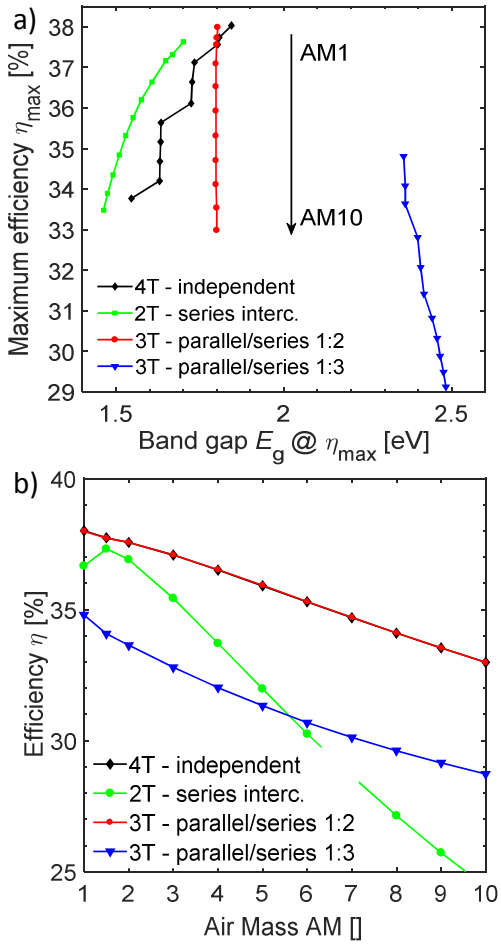

Fig. 4 a) Optimum band gap energies of the top cell and the corresponding maximum efficiency η_{max} for III-V/Si tandem solar cells and b) their efficiency as a function of air mass using different operation modes under AM1G to AM10G spectra with a normalized intensity of 1000 W/m². In b) the band gap energy is constant at the optimal band gap under STC for each configuration.

Fig. 5 shows the impact of varying intensities for the AM1.5G spectra between 100 and 1000 W/m² on the cell performance. The performance decreases for decreasing illumination intensity for all configurations. However, the increased loss in the parallel/series interconnected 3T (1:2) device compared to the 4T device occurs mainly for low intensities. Again, both of these configurations outperform the 2T case.

Combining the effects of spectral changes and intensity for AM1G to AM10G spectra, and assuming for each configuration the optimal band gap under AM1.5G, leads to similar results as for the normalized spectra. Especially, the parallel/series interconnected 3T devices still perform as well as operating the subcells independently (4T).

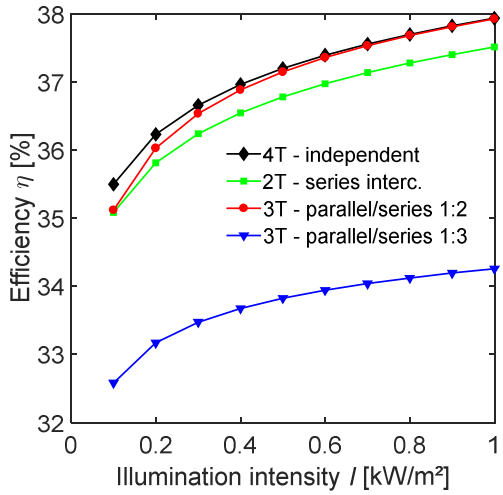

Fig. 5 Efficiency for III-V/Si tandem solar cells as a function of illumination intensity using AM1.5G spectrum. The band gaps of the top cells are fixed to their optimal band gaps at 1000 W/m².

To model the performance of tandem devices with different numbers of terminals under outdoor spectra, we integrated the annual energy yield using the spectral data of the typical metrological year (TMY) for Denver, Colorado, USA [24]. Table I shows the energy yield divided by the total incoming irradiation, assuming a constant temperature of 25°C.

TABLE I
ANNUAL EFFICIENCY CALCULATED FOR DIFFERENT BAND GAP ENERGIES WITH THE SPECTRAL TMY DATA FOR DENVER, CO, USA.

Number of terminals	1.42 eV	1.67 eV	1.81 eV
2	20.4%	35.4%	33.0%
3	31.6%	35.4%	36.3%
4	33.3%	35.9%	36.4%

E_g = 1.42 eV is the band gaps of GaAs, E_g = 1.81 eV the band gap of GaInP, which is also the optimal band gap for the independent operation under AM1.5G and E_g = 1.67 eV the optimal band gap for series interconnected subcells. 3 terminals refers to the parallel/series interconnected 3T (1:2) device.

For all terminal configurations, using a GaAs top cell (E_g = 1.42 eV) performs worst under these varying conditions and a constant W_{oc} = 0.4 eV for all band gaps, despite having the highest demonstrated efficiency under standard test conditions [1]. Using a top cell with the optimal band gap for

Pursuant to the DOE Public Access Plan, this document represents the authors' peer-reviewed, accepted manuscript. The published version of the article is available from the relevant publisher.

the 2T configuration under AM1.5G ($E_g = 1.67$ eV), the parallel/series interconnected 3T (1:2) and series interconnected 2T devices perform equally with 35.4% energy yield. The independent operation (4T) reaches for $E_g = 1.67$ eV 35.9%. This can be increased to 36.4% for 4T and its optimal band gap under AM1.5G of 1.81 eV, which is the band gap of GaInP. Again, the parallel/series interconnected 3T (1:2) device reaches similar high results with 36.3% as the 4T device, where part of the difference can be explained by the slightly non-optimal band gap for the 3T configuration.

B. *Changes in temperature*

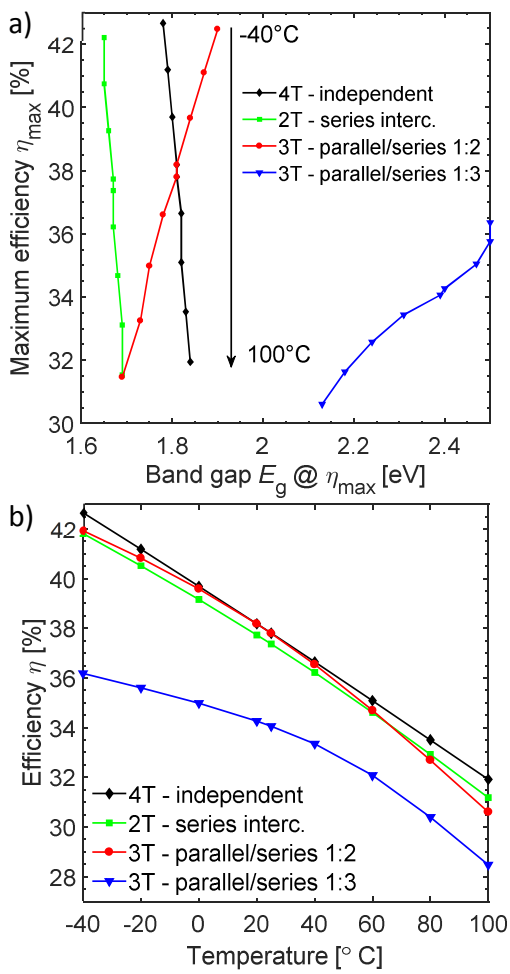

Fig. 6 a) Optimum band gaps of the top cell and the corresponding maximum efficiency η_{max} for III-V/Si tandem solar cells and b) their efficiency as a function of temperature. In b) the band gap energy is constant at the optimal band gap under STC for each configuration.

In contrast to the previous results, the temperature dependence is more pronounced for parallel/series interconnected 3T devices. This is caused by the requirement of voltage matching, in contrast to series interconnect devices, which need to be current matched. Fig. 6 a) shows that for the independent operation and series interconnected case, the changes in the optimal band gap are about 0.05 eV. However, for 3T devices, it is 0.21 eV for a ratio 1:2 and more than 0.4 eV for 1:3.

As indicated in Fig. 6 b), the 3T (1:2) devices perform as well as independent subcell operation only at the temperature the band gaps were optimized for, e.g. 25°C. Nevertheless, for the majority of realistic operation temperatures (up to 60°C) [25] the parallel/series interconnected 3T (1:2) devices still perform better than series interconnected tandems.

C. *Changes in series resistance*

A change in series resistance of the individual cells mainly affects the voltages at maximum power point, with less impact on current. Therefore, we analyzed the effect by series resistance contributions on the operation of the parallel/series interconnected 3T (1:2) device. We compare the effect to the efficiency reduction of the independent operation of the subcells, to differentiate the effect due to voltage mismatch. The analysis in Fig. 7 shows that for series resistance values of up to 500 mΩ cm² for the bottom cells, the efficiency losses of the parallel/series interconnected 3T (1:2) devices are marginal (about 0.1%$_{abs}$) compared to the independent operation of the subcells. The effect of the bottom cells is about twice as severe as of the top cell, since two bottom cells are interconnected in parallel to one top cell.

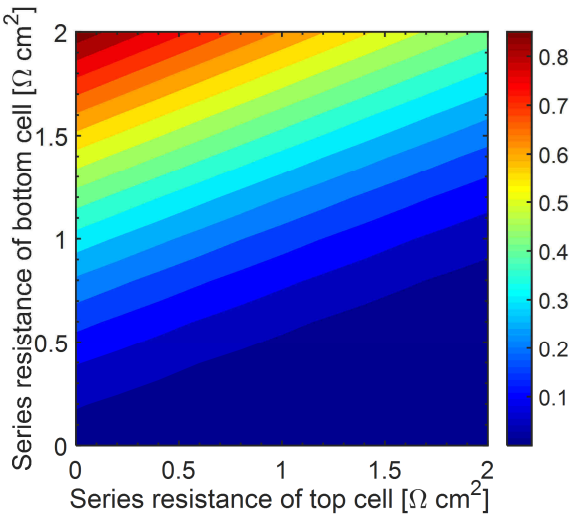

Fig. 7 Absolute efficiency loss [%abs] under STC of parallel/series interconnected 3T (1:2) devices compared to independently operated subcells as a function of the series resistances of the subcells. The band gap of the top cells is fixed at 1.81 eV.

IV. Conclusion

We showed that in the case of top cells with an band gap of $E_g = 1.81$ eV (GaInP) on silicon bottom cells ($E_g = 1.12$ eV), parallel/series interconnected 3T (1:2) devices perform as well as operating the top and bottom cell individually under STC

Pursuant to the DOE Public Access Plan, this document represents the authors' peer-reviewed, accepted manuscript. The published version of the article is available from the relevant publisher.

and most operation conditions. As a consequence, modules with 3T (1:2) devices integrated in one circuit have the potential to reach similar power as modules with separate circuits for the top and bottom cells of 4T devices. This holds also under varying spectra between AM1G to AM10G and the annual yield. Other 3T devices, where the ratio of the number of bottom cells to the number of top cells interconnected in parallel is an integer (1:1 and 1:3), show a significantly reduced performance.

Depending on the spectra, the advantage of parallel/series interconnected 3T devices compared to series interconnected 2T devices is up to $8\%_{abs}$ when choosing the band gap of the top cell to be the optimum under STC (parallel/series interconnected 3T devices (1:2): 1.8 eV, series interconnected 2T devices: 1.7 eV) under the assumption of no interconnection losses and infinite strings. Only in the case of high operation temperatures (> 60°C) do series interconnected devices perform better than parallel/series interconnected ones, when both top cells are optimized for STC. However, this temperature limit can be shifted to higher values by optimizing the band gap of the top cell for higher temperatures. Additionally, we showed that series resistance contributions have only a marginal effect on the performance of parallel/series interconnected 3T devices relative to the independent operation of the subcells.

Therefore, we conclude that modules with parallel/series interconnected tandem devices are much more robust against changes to the operation conditions than series interconnected devices for a wide range of top cell's band gaps including GaAs and GaInP. They reach similar high efficiencies as the independent operation of the subcells. Thus, they offer a promising way to enable the integration of monolithic tandem cells into modules at comparable high efficiency as 4T devices that require in general two separate devices with additional metallization layers between the two junctions.

ACKNOWLEDGMENT

The authors thank Emily L. Warren (NREL), Manuel Schnabel (NREL), Paul Stradins (NREL), M. Rienäcker (ISFH), S. McAlpine (NREL), Myles Steiner (NREL) and U. Römer (UNSW) for fruitful discussions. The U.S. Government retains and the publisher, by accepting the article for publication, acknowledges that the U.S. Government retains a nonexclusive, paid up, irrevocable, worldwide license to publish or reproduce the published form of this work, or allow others to do so, for U.S. Government purposes.

REFERENCES

[1] S. Essig, C. Allebé, T. Remo, J. F. Geisz, M. A. Steiner, K. Horowitz, L. Barraud, J. S. Ward, M. Schnabel, A. Descoeudres, D. L. Young, M. Woodhouse, M. Despeisse, C. Ballif, and A. Tamboli, "Raising the one-sun conversion efficiency of III–V/Si solar cells to 32.8% for two junctions and 35.9% for three junctions," *Nat. Energy*, vol. 2, no. 9, p. 17144, 2017.

[2] J. M. Gee, "A comparison of different module configurations for multi-band-gap solar cells," *Solar Cells*, vol. 24, no. 1-2, pp. 147–155, 1988.

[3] T. Trupke and P. Würfel, "Improved spectral robustness of triple tandem solar cells by combined series/parallel interconnection," *J. Appl. Phys.*, vol. 96, no. 4, p. 2347, 2004.

[4] I. Almansouri, A. Ho-Baillie, S. P. Bremner, and M. A. Green, "Supercharging Silicon Solar Cell Performance by Means of Multijunction Concept," *IEEE J. Photovoltaics*, vol. 5, no. 3, pp. 968–976, 2015.

[5] S. Essig, J. F. Geisz, M. A. Steiner, A. Merkle, R. Peibst, J. Schmidt, R. Brendel, S. Ward, D. J. Friedman, P. Stradins, and D. L. Young, "Development of highly-efficient GaInP/Si Tandem Solar Cells," in *42nd IEEE Photovoltaic Specialists Conference*, 2015, pp. 1–4.

[6] E. L. Warren, M. G. Deceglie, M. Rienäcker, R. Peibst, A. C. Tamboli, and P. Stradins, "Maximizing tandem solar cell power extraction using a three-terminal design," *Energy Environ. Sci.*, submitted, 2017.

[7] M. Rienäcker, E. L. Warren, M. Schnabel, H. Schulte-Huxel, A. Merkle, S. Kajari-Schröder, R. Niepelt, R. Brendel, P. Stradins, A. C. Tamboli, and R. Peibst, "Maximum Power Extraction Enabled by Monolithic Tandems Using Interdigitated Back Contact Bottom Cells with Three Terminals," *Prog. Photovolt: Res. Appl.*, to be submitted, 2017.

[8] H. Liu, Z. Ren, Z. Liu, A. G. Aberle, T. Buonassisi, and I. M. Peters, "The realistic energy yield potential of GaAs-on-Si tandem solar cells: a theoretical case study," *Optics express*, vol. 23, no. 7, A382-90, 2015.

[9] R. Strandberg, "Detailed balance analysis of area de-coupled double tandem photovoltaic modules," *Appl. Phys. Lett.*, vol. 106, no. 3, p. 33902, 2015.

[10] A. L. Lentine, G. N. Nielson, M. Okandan, W. C. Sweatt, J. L. Cruz-Campa, and V. Gupta, "Optimal cell connections for improved shading, reliability, and spectral performance of microsystem enabled photovoltaic (MEPV) modules," in *35th IEEE Photovoltaic Specialists Conference*, 2010, pp. 3048–3054.

[11] J. C. Jimeno, J. R. Gutierrez, V. Fano, C. del Canizo, A. Habib, M. A. Rasool, and A. Otaegi, "Upgrading the silicon IBC to the 40% efficiency," in *43rd IEEE Photovoltaic Specialists Conference*, 2016, pp. 651–656.

[12] S. MacAlpine, D. C. Bobela, S. Kurtz, M. P. Lumb, K. J. Schmieder, J. E. Moore, R. J. Walters, and K. Alberi, "Simulated potential for enhanced performance of mechanically stacked hybrid III–V/Si tandem photovoltaic modules using DC–DC converters," *J. Photon. Energy*, vol. 7, no. 04, p. 1, 2017.

[13] H. Schulte-Huxel, E. L. Warren, M. Schnabel, P. Stradins, D. J. Friedman, and A. Tamboli, "III-V/Si tandem cell to module interconnection – comparison between different operation modes," in *44th IEEE Photovoltaic Specialists Conference*, 2017.

[14] R. M. France, J. F. Geisz, M. A. Steiner, D. J. Friedman, J. S. Ward, J. M. Olson, W. Olavarria, M. Young, and A. Duda, "Pushing Inverted Metamorphic Multijunction Solar Cells Toward Higher Efficiency at Realistic Operating Conditions," *IEEE J. Photovoltaics*, vol. 3, no. 2, pp. 893–898, 2013.

[15] R. R. King, D. Bhusari, A. Boca, D. Larrabee, X.-Q. Liu, W. Hong, C. M. Fetzer, D. C. Law, and N. H. Karam, "Band gap-voltage offset and energy production in next-generation multijunction solar cells," *Prog. Photovolt: Res. Appl.*, vol. 19, no. 7, pp. 797–812, 2011.

[16] J. F. Geisz, M. A. Steiner, I. García, S. R. Kurtz, and D. J. Friedman, "Enhanced external radiative efficiency for 20.8% efficient single-junction GaInP solar cells," *Appl. Phys. Lett.*, vol. 103, no. 4, p. 41118, 2013.

[17] J. C. Fan, "Theoretical temperature dependence of solar cell parameters," *Solar Cells*, vol. 17, no. 2-3, pp. 309–315, 1986.

[18] V. Alex, S. Finkbeiner, and J. Weber, "Temperature dependence of the indirect energy gap in crystalline silicon," *Journal of Applied Physics*, vol. 79, no. 9, pp. 6943–6946, 1996.

[19] I. Vurgaftman, J. R. Meyer, and L. R. Ram-Mohan, "Band parameters for III–V compound semiconductors and their alloys," *Journal of Applied Physics*, vol. 89, no. 11, pp. 5815–5875, 2001.

Pursuant to the DOE Public Access Plan, this document represents the authors' peer-reviewed, accepted manuscript. The published version of the article is available from the relevant publisher.

[20] B. Schumann, *Properties of Gallium Arsenide. EMIS Datareviews Series no. 2, second edition. INSPEC, The Institute of Electric Engineering, London and New York,* 1991.

[21] C. Schinke, P. Christian Peest, J. Schmidt, R. Brendel, K. Bothe, M. R. Vogt, I. Kröger, S. Winter, A. Schirmacher, S. Lim, H. T. Nguyen, and D. MacDonald, "Uncertainty analysis for the coefficient of band-to-band absorption of crystalline silicon," *AIP Advances*, vol. 5, no. 6, p. 67168, 2015.

[22] C. A. Gueymard, "Parameterized transmittance model for direct beam and circumsolar spectral irradiance," *Solar Energy*, vol. 71, no. 5, pp. 325–346, 2001.

[23] C. A. Gueymard, "SMARTS, A Simple Model of the Atmospheric Radiative Transfer of Sunshine: Algorithms and Performance Assessment." *Professional Paper FSEC-PF-270-95. Florida Solar Energy Center, 1679 Clearlake Rd., Cocoa, FL 32922.*

[24] NREL, *National Solar Radiation Database (NSRDB).* [Online] Available: https://maps.nrel.gov/nsrdb-viewer.

[25] J. Haschke, J. P. Seif, Y. Riesen, A. Tomasi, J. Cattin, L. Tous, P. Choulat, M. Aleman, E. Cornagliotti, A. Uruena, R. Russell, F. Duerinckx, J. Champliaud, J. Levrat, A. A. Abdallah, B. Aïssa, N. Tabet, N. Wyrsch, M. Despeisse, J. Szlufcik, S. de Wolf, and C. Ballif, "The impact of silicon solar cell architecture and cell interconnection on energy yield in hot & sunny climates," *Energy Environ. Sci.*, vol. 9, p. 2122, 2017.

Pursuant to the DOE Public Access Plan, this document represents the authors' peer-reviewed, accepted manuscript. The published version of the article is available from the relevant publisher.